Published in final edited form as:

Nat Med. 2005 November ; 11(11): 1180–1187. doi:10.1038/nm1303.

CCL5-CCR5 interaction provides antiapoptotic signals for macrophage survival during viral infection

Jeffrey W Tyner[1], **Osamu Uchida**[1], **Naohiro Kajiwara**[1], **Edy Y Kim**[1], **Anand C Patel**[2], **Mary P O'Sullivan**[1], **Michael J Walter**[1], **Reto A Schwendener**[3], **Donald N Cook**[4], **Theodore M Danoff**[5], and **Michael J Holtzman**[1,6]

[1]Department of Medicine, Washington University School of Medicine, 660 South Euclid Avenue, St. Louis, Missouri 63110, USA.

[2]Department of Pediatrics, Washington University School of Medicine, 660 South Euclid Avenue, St. Louis, Missouri 63110, USA.

[3]Department of Molecular Cell Biology, Paul Scherrer Institute, Villigen, Switzerland CH-5232.

[4]Department of Medicine, Duke University School of Medicine, Durham, North Carolina 27710, USA.

[5]Department of Medicine, University of Pennsylvania School of Medicine, Philadelphia, Pennsylvania 19104, USA.

[6]Department of Cell Biology, Washington University School of Medicine, 660 South Euclid Avenue, St. Louis, Missouri 63110, USA.

Abstract

Host defense against viruses probably depends on targeted death of infected host cells and then clearance of cellular corpses by macrophages. For this process to be effective, the macrophage must presumably avoid its own virus-induced death. Here we identify one such mechanism. We show that mice lacking the chemokine Ccl5 are immune compromised to the point of delayed viral clearance, excessive airway inflammation and respiratory death after mouse parainfluenza or human influenza virus infection. Virus-inducible levels of Ccl5 are required to prevent apoptosis of virus-infected mouse macrophages *in vivo* and mouse and human macrophages *ex vivo.* The protective effect of Ccl5 requires activation of the Ccr5 chemokine receptor and consequent bilateral activation of $G_{\alpha i}$-PI3K-AKT and $G_{\alpha i}$-MEK-ERK signaling pathways. The antiapoptotic action of chemokine signaling may therefore allow scavengers to finally stop the host cell-to-cell infectious process.

The host response to intracellular pathogens is aimed at rapidly killing infected cells. In the case of respiratory viruses, host cells may be programmed with innate responses triggering

Correspondence should be addressed to M.J.H. (holtzman@im.wustl.edu).

Note: Supplementary information is available on the Nature Medicine website.

COMPETING INTERESTS STATEMENT

The authors declare that they have no competing financial interests.

cell suicide and immune cell recruitment and activation[1]. For effective control of infection, the host must also mount an adaptive immune response that depends primarily on cytotoxic lymphocytes[2]. These cells are guided to the tissue by local expression of cell adhesion molecules and chemokines provided by infected cells[3–5]. Once at the site, T-cell recognition of infected cells triggers killing, thus eliminating these target cells[6]. This process may be mutually reinforcing, as it seems that chemokines such as chemokine (C-C motif) ligand 5 (CCL5) may not only recruit cytotoxic lymphocytes but may also aid in the generation and activation of antigen-specific T cells[7–9].

Once this killing phase is complete, it is equally crucial to clear virus-infected, apoptotic cells from the tissue. The cell type responsible for clearance of debris is primarily the tissue macrophage. If the clearance process is disrupted, pathogens are not effectively removed and residual apoptotic cells, including activated macrophages themselves, can cause further tissue damage through proinflammatory proteinases and cytokines. Thus, for effective clearance to take place, macrophage viability must be maintained in the face of infection. The basis for the preservation of infected macrophages is poorly understood.

Here, we assess the role of Ccl5 in antiviral immunity using experimental viral infection and a mouse that lacks Ccl5 (*Ccl5*$^{-/-}$). Based on earlier work[3,5], we expected to find a defect in immune cell traffic, consistent with the phenotype of other chemokine-deficient mice[10,11]. Instead, we show that Ccl5 is essential to protect tissue macrophages from virus-inducible cell death, thus allowing them to clear the infection. This chemokine function is dependent on chemokine (C-C motif) receptor 5 (Ccr5) activation at physiologic levels of ligand that stimulate the antiapoptotic cascade pathways $G_{\alpha i}$–phosphatidylinositol-3-kinase (PI3K)–AKT and $G_{\alpha i}$–mitogen-activated protein kinase kinase (MEK)–extracellular-signal-regulated kinase-1/2 (ERK1/2), which mediate cell growth and survival in other systems[12,13].

RESULTS

Effect of viral infection on *Ccl5*$^{-/-}$ and *Ccr5*$^{-/-}$ mice

We assessed the pattern of expression and function of Ccl5 in *Ccl5*$^{-/-}$ versus wild-type mice inoculated with mouse parainfluenza virus type 1 Sendai virus (SeV). The experimental conditions allowed for high viral replication and a pattern of infection and illness in wild-type C57BL6/J mice that was similar to human paramxyovirus infection[1,14]. In response to replicating SeV, *Ccl5* mRNA and protein were induced in the lungs of wild-type but not *Ccl5*$^{-/-}$ mice (Fig. 1a). Ccl5 was expressed predominantly in airway epithelial cells, closely matching the major sites of viral replication (Fig. 1a and Supplementary Fig. 1 online). Both *Ccl5*$^{-/-}$ mice and *Ccr5*$^{-/-}$ mice showed increased lethargy, weight loss and mortality after infection compared to wild-type mice (Fig. 1b). In infected wild-type mice *Ccr5* (but not the genes encoding other Ccl5 receptors such as Ccr1 and Ccr3) was induced in airway epithelial cells and macrophages, again tracking with viral replication (Fig. 1c,d and Supplementary Fig. 1 online). Under all conditions, necropsy indicated bronchiolitis and alveolitis without abnormalities in organs other than the lung.

We initially reasoned that the decreased survival of *Ccl5*$^{-/-}$ and *Ccr5*$^{-/-}$ mice could result from abnormalities in T-cell function[5,7], but we observed no differences in airway lymphocyte infiltration in *Ccl5*$^{-/-}$ and *Ccr5*$^{-/-}$ mice compared to wild-type mice (Fig. 2a). Moreover, flow cytometry of immune cells from spleen, lung, and bronchoalveolar lavage (BAL) fluid of *Ccl5*$^{-/-}$ and wild-type mice showed that levels of T-cell activation seemed unchanged. In particular, SeV infection caused similar increases in CD8$^+$ SeV-specific, as well as total CD8$^+$, CD25$^+$, CD44$^+$ and interferon (IFN)-γ^+ lymphocytes and similar decreases in CD62L$^+$ lymphocytes in *Ccl5*$^{-/-}$ and wild-type mice (Fig. 2b, Supplementary Fig. 2 online and data not shown). Thus, virus-inducible T-cell activation and traffic seemed to be intact despite the *Ccl5* deficiency. In contrast, *Ccl5*$^{-/-}$ mice showed a decrease in macrophage numbers in the airspace concomitant with an accumulation of macrophages in the subepithelium at days 4–7 after infection and epithelium at days 8–9 after infection (Fig. 2a,c and Supplementary Fig. 3 online). Immunostaining of serial tissue sections and lung and BAL fluid cells indicated that these macrophages were persistently infected with virus and were undergoing apoptosis at increased levels in *Ccl5*$^{-/-}$ compared to wild-type mice (Fig. 2c–e and Supplementary Fig. 3 online). The same pattern was found in *Ccr5*$^{-/-}$ mice (data not shown). Using a more common human pathogen, influenza virus (FluV), we found a similar compromise in *Ccl5*$^{-/-}$ and *Ccr5*$^{-/-}$ mice, including increased death rates and accumulation of infected, apoptotic tissue macrophages (Supplementary Fig. 4 online). Thus, our results suggested an alteration in macrophage behavior underlying the phenotype of *Ccl5*$^{-/-}$ mice.

Ccl5-Ccr5 interaction and macrophage survival

The phenotype we observed in *Ccl5*$^{-/-}$ mice was distinct from those found in other models of chemokine blockade, in which animals show decreased immune cell emigration after infection[10,11,14,15]. Our results may have been compatible with defective macrophage traffic due to loss of chemotactic signal, resulting in higher levels of macrophage infection and death; however, the distinct phenotype in *Ccl5*$^{-/-}$ mice was better explained when we found that the Ccl5-Ccr5 interaction was necessary to prevent virus-induced apoptosis in isolated macrophages.

Initial experiments indicated that wild-type mouse macrophages inoculated with SeV highly induced *Ccl5* mRNA. Levels of mRNA encoding the Ccl5 receptors (Ccr1, Ccr3, Ccr5) or alternative ligands for these receptors (Ccl3, Ccl4) were unchanged by viral infection (Fig. 3a). Macrophages from *Ccl5*$^{-/-}$ mice did not induce *Ccl5* in response to viral infection, but otherwise showed similar expression of genes encoding other chemokines, chemokine receptors and antiviral proteins (Fig. 3b and data not shown). Macrophages from wild-type mice achieved Ccl5 levels of 5–8 nM in culture medium by days 2–4 after inoculation (Fig. 3b) and also upregulated Ccr5 (Fig. 3a,c and Supplementary Fig. 5 online), similar to the expression pattern found *in vivo*. Induction of Ccr5 protein without corresponding increases in *Ccr5* mRNA is consistent with reports that the expression of chemokine receptors is regulated at the level of protein traffic to the cell surface[16,17].

Under these conditions, endogenous Ccl5 was protective against virus-induced apoptosis (Fig. 3d and Supplementary Fig. 5 online). Moreover, exogeneous restoration of physiologic

levels of Ccl5 fully reversed the defect in cells from *Ccl5*$^{-/-}$ mice. In addition, the absence or blockade of Ccr5 caused increased virus-inducible apoptosis at levels equivalent to those observed in *Ccl5*$^{-/-}$ macrophages (Fig. 3d). Thus, in *Ccl5*$^{-/-}$ and *Ccr5*$^{-/-}$ mice, accumulation of apoptotic macrophages in tissue could be explained by premature cell death before reaching the airspace. In addition, similar to findings with mouse macrophages, we found that blockade of Ccr5 caused increased apoptosis in human macrophages infected with SeV as well as respiratory syncytial virus and influenza virus (Fig. 3e).

Ccl5-Ccr5 interaction inhibits virus-induced apoptosis

We next aimed to determine how Ccl5 and Ccr5 protected against virus-induced apoptosis. Ccl5 inhibition of viral entry and/or replication seemed improbable, as similar infection rates (95–100%) were seen in wild-type and *Ccl5*$^{-/-}$ cells, and viral replication was similar in macrophages with or without Ccl5 (Fig. 3f). Additional experiments indicated that initial rates of infection were also no different at lower multiplicity of infection (MOI; 0.1–10) in wild-type versus *Ccl5*$^{-/-}$ cells (data not shown). Instead, our results indicate that Ccl5 blocks virus-inducible apoptosis in macrophages through inhibiting intracellular death pathways. Accordingly, we defined the Ccl5-triggered signaling pathway that blocks virus-induced apoptosis using a combined analysis of phosphorylation and activation events and corresponding levels of apoptosis in the presence or absence of selective inhibitors.

Initial experiments indicated that Ccl5 induced the phosphorylation of Erk1/2 and Akt in mouse and human macrophages. This was dependent on ligand concentration, blocked by Ccl5- or Ccr5-specific antibodies, and was absent in *Ccr5*$^{-/-}$ macrophages (Fig. 4a and data not shown). In particular, Ccl5 concentrations in the range detected during viral infection (0.1–10 nM) activated Erk1/2 and Akt through a mechanism that depended on Ccr5 (Fig. 4a). We found a similar pattern of activation for Ccl3 and Ccl4 (Supplementary Fig. 6 online), suggesting that the basis for the *Ccl5*$^{-/-}$ phenotype rests on the selective virus-inducible expression of Ccl5 rather than distinct signaling capabilities. Treatment with concentrations of Ccl5 greater than the physiologic range (100 nM) caused further activation of Erk1/2 that did not depend on Ccr5. This finding is consistent with reports of Ccl5 multimer formation at higher concentrations that bind cell-surface glycosaminoglycans and activate SRC kinase-dependent signaling[18].

As Ccl5 showed antiapoptotic function at low (2–10 nM) levels that required Ccr5, we first concentrated on defining signaling through this interaction. At low concentrations (5 nM), CCL5-inducible activation of ERK (but not AKT) was blocked by the MEK inhibitor PD98059, whereas activation of AKT (but not ERK) was blocked by the PI3K inhibitor LY294002 in human macrophages (Fig. 4b,c), at least partially segregating these two CCL5-CCR5–driven pathways. We inhibited each of these pathways by treatment with pertussis toxin, which inhibits the G protein downstream of CCR5 and upstream of MEK-ERK and PI3K-AKT (Fig. 4b,c). As pertussis toxin also increased background phosphorylation, we also tested it in combination with LY294002 (which decreased background) and still found inhibition of MEK-ERK signaling. Neither of these pathways (CCR5-$G_{\alpha i}$-MEK-ERK or CCR5-$G_{\alpha i}$-PI3K-AKT) was influenced by the SRC kinase inhibitors herbimycin A or PP2. When we administered CCL5 at high (100 nM) levels, inducible activation of ERK1/2 (but

not AKT) was further increased, and this activation persisted despite treatment with pertussis toxin and was sensitive to herbimycin A (Supplementary Fig. 6 online). These findings suggest SRC-dependent (CCR5- and G-protein-independent) activation of ERK1/2 at higher levels of CCL5 in macrophages. This level of CCL5 is somewhat less than reported for herbimycin-sensitive effects in T-cell clones (1 μM)[7], but seems still capable of activating the hematopoietic cell kinase (HCK) member of the SRC kinase family[18] (Supplementary Fig. 6 online).

Together, our observations indicate that high levels of CCL5 (capable of multimer formation) signal through HCK independently of the CCR5 G-protein-coupled receptor, but at physiologic levels, CCL5 (acting as a monomer) signals through CCR5 and independently of any SRC family kinases. In this case, CCR5 activation initiates dual signals to $G_{\alpha i}$-MEK-ERK or $G_{\alpha i}$-PI3K-AKT. Consequently, losing either of these two pathways should lead to loss of protection from virus-induced apoptosis. This possibility was confirmed when we observed that inhibition of either Akt or Erk pathways (under conditions not affecting baseline apoptosis) caused substantial increases in virus-induced apoptosis in wild-type but not *Ccl5*$^{-/-}$ macrophages (Fig. 4d).

We reasoned the same antiapoptotic pathways observed in macrophages might be present in airway epithelial cells, because these cells also showed viral induction of *Ccl5* and *Ccr5* expression *in vivo*. This prediction was confirmed when we observed increases in virus-induced apoptosis, accompanied by caspase dependence and mitochondrial membrane depolarization, in *Ccl5*$^{-/-}$ and *Ccr5*$^{-/-}$ airway epithelial cells *in vitro* (Supplementary Fig. 7 online). Together, the findings define a pathway for virus-inducible apoptosis that relies on caspase activation and mitochondrial dysfunction and is ordinarily held in check by Ccl5 and Ccr5 expression and signaling.

Defective signaling and macrophage function *in vivo*

We aimed to further link our observations *in vivo* with those *in vitro*. We initially analyzed signaling events in cells obtained by BAL from *Ccl5*$^{-/-}$ versus wild-type mice after viral infection. Similar to our observations in cultured macrophages, we found that *Ccl5*$^{-/-}$ and wild-type mice manifest similar activation of Erk1/2 and Akt at baseline, but *Ccl5*$^{-/-}$ mice showed blunted activation after viral infection (Fig. 5a). Differences were maximal at days 3–5 and were absent by day 8 after inoculation, thus coinciding with the time course for Ccl5 expression. We attributed decreased phosphorylation in *Ccl5*$^{-/-}$ BAL cells to the predominant macrophage population, but recognized that other cell types could influence the results. Accordingly, we monitored kinase activation by immunostaining of BAL fluid cells and tissue sections and found that *Ccl5*$^{-/-}$ macrophages showed a notable decrease in levels of phosphorylated Erk1/2 and phosphorylated Akt after viral infection (Fig. 5b-d). We also found that *Ccl5*$^{-/-}$ mice showed decreased expression of the Erk-dependent c-fos family of transcription factors by day 8 after inoculation (Fig. 5e,f). Accordingly, we detected viral induction of c-fos family members (especially fos-like antigen 1) in wild-type but not *Ccl5*$^{-/-}$ cells in culture (Supplementary Fig. 7 online).

Next we tested whether macrophage depletion was sufficient to reproduce the pathology predicted by loss of macrophage antiapoptotic signaling in the *Ccl5*$^{-/-}$ phenotype.

Accordingly, we depleted macrophages in wild-type mice during SeV infection using clodronate liposomes. We found a marked and selective decrease in macrophage infiltration at the site of infection (Fig. 6a,b). Furthermore we found evidence of persistent virus in macrophage-depleted mice at late time points (day 9) despite similar viral replication in macrophage-depleted and control mice at early time points (days 1–7; Fig. 6a,c), correlating precisely with the pattern in *Ccl5*$^{-/-}$ and *Ccr5*$^{-/-}$ mice. Similarly, macrophage-depleted and control mice developed similar levels of apoptotic epithelial cells at day 7, but only macrophage-depleted mice retained apoptotic cells by day 9 (Fig. 6a,d). Persistent viral infection was accompanied by airway inflammation that led to death in a percentage of mice similar to the rate for *Ccl5*$^{-/-}$ mice with or without clodronate liposome treatment (Fig. 6e). In particular, macrophage depletion in *Ccl5*$^{-/-}$ mice caused no further mortality beyond macrophage depletion in wild-type mice. Thus, the phenotype for macrophage-deficient mice follows closely the one predicted for defects in *Ccl5*$^{-/-}$ and *Ccr5*$^{-/-}$ mice (*i.e.*, decreased clearance of virus and apoptotic, infected cells and concomitant decrease in survival from respiratory compromise). Moreover, wild-type and *Ccl5*$^{-/-}$ mice no longer showed differences in survival if both were depeleted of macrophages. These findings provide the basis for a heretofore undefined requirement for macrophage-dependent clearance of virus-infected cells that could be sufficient to explain the observed immune compromise in the setting of viral infection.

DISCUSSION

Host defense against intracellular pathogens is traditionally defined by innate and adaptive immune responses aimed at death of infected cells. Chemokines and macrophages influence both arms of the immune response[7,19,20], so it is not surprising that in other models of infection, loss of chemokine expression results in decreased immune cell recruitment[10,11]. Based on this anti-inflammatory action, chemokine antagonism has been offered as a therapeutic approach for inflammatory diseases[21]. CCR5 signaling has also been targeted for specific blockade based on the ability of CCR5 to serve as a viral coreceptor[22,23].

Here we show that the chemokine of Ccl5 also has a distinct role in host defense based on Ccl5-Ccr5 activation of G-protein-dependent PI3K-AKT and MEK-ERK signaling pathways that are essential to inhibit apoptosis of virus-infected cells. Ordinarily, apoptosis of infected cells is helpful for host defense[24], but the present paradox whereby increased apoptosis is harmful to the host may be explained by the crucial role of infected macrophages in resisting cell death and so efficiently clearing virus-infected, apoptotic cells from the tissue. If this clearance process is disrupted, pathogens are not effectively removed and residual apoptotic cells, including activated macrophages, can cause further tissue damage. Because of the widespread role for the macrophage in host defense, Ccl5-Ccr5 influence on cell death may be crucial for effective clearance of a wide range of intracellular pathogens. Our insights may therefore hold value for susceptibility to infection and specifically for respiratory viral infection, given that paramyxoviruses and influenza viruses are common causes of serious respiratory infection and major influences on chronic respiratory disease[25–28].

Our results also help to address how intracellular signaling can be tailored to host defense against specific pathogens. Thus, viral infection selectively promotes expression of Ccl5 (but

not Ccl3 or Ccl4) as ligand and Ccr5 (but not Ccr1 or Ccr3) as corresponding receptor. Whereas expression of the *Ccl5* gene is controlled by transcriptional and post-transcriptional mechanisms[5], *Ccr5* mRNA is uninfluenced by viral infection so that expression of Ccr5 protein may depend on increased translation or accelerated transport of Ccr5 to the cell surface. In either case, our findings show the host can coordinate expression of Ccl5 and Ccr5 at the site of viral replication to promote an efficient antiviral defense. These distinct regulatory mechanisms of gene expression also explain why other receptor-ligand combinations cannot compensate for *Ccl5* and/or *Ccr5* deficiency despite their ability to activate PI3K-AKT and MEK-ERK antiapoptotic signals.

Finally, our results also help to resolve the role of CCL5 concentration on cellular responses. CCL5 has been found to act on T cells as a chemoattractant at low (nanomolar) levels and an activator at high (micromolar) levels[7]. Whether these higher concentrations are functional *in vivo* remains uncertain. Thus, *Ccl5*$^{-/-}$ mice develop fewer antigen-specific T cells during the delayed-type hypersensitivity response to keyhole limpet hemocyanin (KLH)[9] but generate normal levels of virus-specific T cells in response to viral infection. In both settings, tissue infiltration by macrophages is abnormal, perhaps underscoring the role of CCL5 in regulating macrophage behavior. Nonetheless, subsequent reports identified high-level CCL5 multimers binding cell-surface GAGs and triggering SRC kinase-dependent activation of ERK in transformed cell lines[18]. Our results indicate that CCL5 activates a similar pattern of SRC-ERK signals in primary macrophages. But the same downstream signal is derived from low-level monomeric CCL5 interacting with CCR5 and so still helps to protect against virus-induced apoptosis. Moreover, CCL5-CCR5 interaction provides an additional PI3K signal that is also necessary for protection against virus-inducible apoptosis. The complex nature of this signaling mechanism (Supplementary Fig. 8 online) thereby allows for distinct effects on different viral pathogens. Indeed, the genetic variability of *CCR5* alleles in humans may reflect ongoing pressure to adapt this system to defend against viral pathogens as diverse as human immunodeficiency virus and paramyxoviruses[22,29]. Whether similar variability exists in CCL5 expression still must be defined, but our results provide a mechanistic basis for predicting how genetic or pharmacologic alterations in CCL5-CCR5 function may influence host defense against common paramyxoviral infections.

METHODS

For details, see Supplementary Methods online.

Generation and treatment of mice.

We generated *Ccl5*$^{-/-}$ and control wild-type mice as described previously[9] and obtained *Ccr5*$^{-/-}$ mice[30] and control C57BL/6J mice from The Jackson Laboratory. We maintained all mice under pathogen-free conditions as described previously[1,14]. For macrophage depletion, we treated mice with 2 mg clodronate-containing or control liposomes[31] given by intraperitoneal injection 3 d before viral inoculation and then 0.5 mg on days 0, 3, 6, 9, 12 and 15 after inoculation with SeV.

Viral inoculation and monitoring.

We obtained SeV (Fushimi Strain), respiratory syncytitial virus (A2 strain), and influenza virus (FluV; H1N1 Strain A/WS/SS) from ATCC and inoculated mice or cell cultures as described previously[1,5,14]. We delivered SeV intranasally at 2×10^5 plaque-forming units (p.f.u.) and FluV at 70 $TCID_{50}$ to induce similar mortality rates in wild-type mice. We monitored viral titer as described previously[1,5,14].

Analysis of mRNA.

We performed *in situ* hybridization using a 0.5-kb *Ccl5* cDNA fragment cloned into pGEM3Zf-1 (Promega) to produce ^{35}S-UTP–labeled sense and antisense cRNA transcripts with the Gemini Riboprobe system (Promega). For oligonucleotide microarray, we converted isolated RNA to cDNA with poly(A)$^+$ control spikes and then fragmented cRNA as described previously[32] and amplified poly(A)$^+$ RNA using RiboAmp (Arcturus) followed by BioArray High Yield RNA Transcript Labeling (Enzo). We hybridized duplicate samples to gene chip U74-A (Affymetrix) and generated CEL data files by MAS 5.0 (Affymetrix). Microarray normalization and analysis were performed using previously described methods[33–36].

Immunohistochemistry.

We immunostained mouse lung for SeV, Mac-3 and Ccl5 as described previously[1,14]. We performed immunofluorescence microscopy using Ccr1-, Ccr3- or Ccr5-specific monoclonal antibodies (Santa Cruz Biotechnology), CD68-specific monoclonal antibody (Serotec)[37] and active caspase 3–specific monoclonal antibody (BD PharMingen) and detected primary antibody binding using Cy3- or FITC-conjugated antibodies (Jackson ImmunoResearch Labs). We performed TUNEL reaction using the ApoTag Plus Fluorescein In Situ Apoptosis Detection kit (Intergen) and Hoechst dye #33342 (Molecular Probes). We also blocked tissue sections with non-immune rabbit serum and incubated them with rabbit antibody to mouse phosphorylated Akt (Cell Signaling Technology) or c-fos family–specific antibody (Santa Cruz Biotechnology) followed by biotinylated donkey antibody to rabbit IgG, streptavidin-conjugated horseradish peroxidase and 3.3′-diaminobenzidine.

Flow cytometry.

We isolated splenocytes and lung immune cells and performed BAL as described previously[1,38,39]. We blocked samples with antibody to mouse CD16 and CD32 (BD Biosciences) and then immunostained with antibody to mouse CD3, CD4, CD19, CD25, CD44, CD62L or isotype control (Pharmingen) or CD8a-specific monoclonal antibody (Caltag Laboratories) conjugated with FITC, PE or PerCP. We performed intracellular cytokine staining with antibody to mouse interleukin (IL)-4 or interferon (IFN)-γ as described previously[38]. We detected specific SeV$^+$ T cells using tetrameric MHC-peptide reagents for SeV nucleoprotein ($NP_{324–332}$) or control ovalbumin peptide (SIINFEKL) complexed with K^b provided by the National Institute of Allergy and Infectious Disease Tetramer Core Facility[40].

Cell culture and immunocytochemistry.

We prepared macrophage cultures from mouse and human peripheral blood by Lympholyte-Mammal (Cedarlane) or Optiprep (Accurate Chemical and Scientific) gradient centrifugation, respectively, and adherence to 8-well Labtek chambers. We inoculated cultures on day 5 with SeV (MOI 0.1–20) or SeV-UV for 1–8 d with or without Ccl5 (Peprotech), goat antibody to mouse Ccr5 (0.4 μg/ml; Santa Cruz Biotechnology), mouse antibody to human CCR5 (50 μg/ml; R&D Systems), LY294002 (5 μM) orPD98059 (25 μM; Calbiochem). For each condition, we immunostained cultures with SeV-specific antibody and CY3-conjugated rabbit antibody to rat IgG or with activated caspase 3–specific antibody and Cy3-conjugated donkey antibody to rabbit IgG (Jackson ImmunoResearch Laboratories), counterstained them with Hoechst 33342, and subjected them to TUNEL. We monitored virus induction of Ccl3, Ccl4 and Ccl5 by ELISA (R&D Systems). For *in vivo* correlation experiments, we collected lung tissue cells and BAL fluid cells in DMEM and subjected them to immunofluorescence microscopy with Mac-3–specific antibody, Ccr5-specific antibody, CD68-specific monoclonal antibody, chicken antibody to SeV (SPHFAS, Inc., Charles River Laboratories), or rabbit antibody to phosphorylated Erk1/2 or phosphorylated Akt (Cell Signaling Technology).

Western blotting.

We serum-starved macrophage cultures for 1 d before incubation with CCL5 with or without pretreatment with pertussis toxin (4 mg/ml), LY294002 (50 μM), PD98059 (25 μM), PP2 (10 μM) or herbimycin A (10 μM; CalBiochem). We subjected cell lysates to western blotting with IgG_{2B} antibody to phosphorylated AKT and rabbit antibody to phosphorylated AKT, mouse IgG_1 antibody to phosphorylated ERK1/2 or mouse IgG_1 antibody to β-actin (Chemicon). We then incubated membranes with goat antibody to mouse IgG or IgG_1 or sheep antibody to rabbit IgG conjugated to horseradish peroxidase (Chemicon), exposed them to enhanced chemiluminescence (ECL) reagent and hyperfilm (Amersham), and subjected them to densitometry.

Statistical analysis.

We assessed values for mouse survival by Kaplan-Meier analysis. We analyzed values for ELISA, TUNEL and drug-versus-vehicle treatment using a one-way analysis of variance (ANOVA) for a factorial experimental design. If significance was achieved by one-way analysis, we performed post-ANOVA comparison of means using Scheffe F test. We analyzed values for BAL cell counts, viral titer and immunostaining using paired *t*-test. Significance level for all analyses was 0.05.

Supplementary Material

Refer to Web version on PubMed Central for supplementary material.

ACKNOWLEDGMENTS

This work was supported by grants from the US National Institutes of Health (Heart, Lung, and Blood Institute), the Martin Schaeffer Fund and the Alan A. and Edith L. Wolff Charitable Trust.

References

1. Walter MJ, Kajiwara N, Karanja P, Castro M & Holtzman MJ IL-12 p40 production by barrier epithelial cells during airway inflammation. J. Exp. Med. 193, 339–352 (2001). [PubMed: 11157054]
2. Doherty PC & Christensen JP Accessing complexity: the dynamics of virus-specific T cell responses. Annu. Rev. Immunol. 18, 561–592 (2000). [PubMed: 10837069]
3. Taguchi M et al. Patterns for RANTES secretion and intercellular adhesion molecule-1 expression mediate transepithelial T cell traffic based on analyses *in vitro* and *in vivo*. J. Exp. Med. 187, 1927–1940 (1998). [PubMed: 9625753]
4. Look DC et al. Direct suppression of Stat1 function during adenoviral infection. Immunity 9, 871–880 (1998). [PubMed: 9881977]
5. Koga T et al. Virus-inducible expression of a host chemokine gene relies on replication-linked mRNA stabilization. Proc. Natl. Acad. Sci. USA 96, 5680–5685 (1999). [PubMed: 10318944]
6. Topham DJ, Tripp RA & Doherty PC CD8+ T cells clear influenza virus by perforin or Fas-dependent processes. J. Immunol. 159, 5197–5200 (1997). [PubMed: 9548456]
7. Bacon KB, Premack BA, Gardner P & Schall TJ Activation of dual T cell signaling pathways by the chemokine RANTES. Science 269, 1727–1730 (1995). [PubMed: 7569902]
8. Lillard JJW, Boyaka PN, Taub DD & McGhee JR RANTES potentiates antigen-specific mucosal immune responses. J. Immunol. 166, 162–169 (2001). [PubMed: 11123289]
9. Makino Y et al. Impaired T cell function in RANTES-deficient mice. Clin. Immunol. 102, 302–309 (2002). [PubMed: 11890717]
10. Cook DN et al. Requirement for MIP-1α for an inflammatory response to viral infection. Science 269, 1583–1585 (1995). [PubMed: 7667639]
11. Lu B et al. Abnormalities in monocyte recruitment and cytokine expression in monocyte chemoattractant protein 1-deficient mice. J. Exp. Med. 187, 601–608 (1998). [PubMed: 9463410]
12. Roux PP & Blenis J ERK and p38 MAPK-activated protein kinases: a family of protein kinases with diverse biological functions. Microbiol. Mol. Biol. Rev. 68, 320–344 (2004). [PubMed: 15187187]
13. Fruman DA & Cantley LC Phosphoinositide 3-kinase in immunological systems. Semin. Immunol 14, 7–18 (2002). [PubMed: 11884226]
14. Walter MJ, Morton JD, Kajiwara N, Agapov E & Holtzman MJ Viral induction of a chronic asthma phenotype and genetic segregation from the acute response. J. Clin. Invest 110, 165–175 (2002). [PubMed: 12122108]
15. Lukacs NW et al. Differential recruitment of leukocyte populations and alteration of airway hyperreactivity by C–C family chemokines in allergic airway inflammation. J. Immunol 158, 4398–4404 (1997). [PubMed: 9127004]
16. Pelchen-Matthews A, Signoret N, Klasse PJ, Fraile-Ramos A & Marsh M Chemokine receptor trafficking and viral replication. Immunol. Rev 168, 33–49 (1999). [PubMed: 10399063]
17. Mellado M, Rodriguez-Frade JM, Manes S & Martinez-A. C Chemokine signaling and functional responses: the role of receptor dimerization and TK pathway activation. Annu. Rev. Immunol 19, 397–421 (2001). [PubMed: 11244042]
18. Chang TL et al. Interaction of the CC-chemokine RANTES with glycosaminoglycans activates a p44/42 mitogen-activated protein kinase-dependent signaling pathway and enhances human immunodeficiency virus type I infectivity. J. Virol 76, 2245–2254 (2002). [PubMed: 11836402]
19. Cyster JG Chemokines and cell migration in secondary lymphoid organs. Science 286, 2098–2102 (1999). [PubMed: 10617422]
20. Gu L et al. Control of T_H2 polarization by the chemokine monocyte chemoattractant protein-1. Nature 404, 407–411 (2000). [PubMed: 10746730]
21. Thelen M Dancing to the tune of chemokines. Nat. Immunol. 2, 129–134 (2001). [PubMed: 11175805]
22. Berger EA, Murphy PM & Farber JM Chemokine receptors as HIV-1 coreceptors: roles in viral entry, tropism, and disease. Annu. Rev. Immunol 17, 657–700 (1999). [PubMed: 10358771]

23. Lalani AS et al. Use of chemokine receptors by poxviruses. Science 286, 1968–1971 (1999). [PubMed: 10583963]
24. Lauber K et al. Apoptotic cells induce migration of phagocytes via caspase-3-mediated release of a lipid attraction signal. Cell 113, 717–730 (2003). [PubMed: 12809603]
25. Domachowske JB & Rosenberg HF Respiratory syncytial virus infection: immune response, immunopathogenesis, and treatment. Clin. Microbiol. Rev. 12, 298–309 (1999). [PubMed: 10194461]
26. Sumino KC et al. Detection of severe human metapneumovirus infection by real-time polymerase chain reaction and histopathological assessment. J. Inf. Dis. 192, 1052–1060 (2005). [PubMed: 16107959]
27. Ungchusak K et al. Probable person-to-person transmission of avian influenza A (H5N1). N. Engl. J. Med 352, 333–340 (2005). [PubMed: 15668219]
28. Holtzman MJ et al. Immunity, inflammation, and remodeling in the airway epithelial barrier: epithelial-viral-allergic paradigm. Physiol. Rev 82, 19–46 (2002). [PubMed: 11773608]
29. Hull J et al. Variants of the chemokine receptor CCR5 are associatd with severe bronchiolitis caused by respiratory syncytial virus. J. Infect. Dis 188, 904–907 (2003). [PubMed: 12964123]
30. Tran EH, Kuziel WA & Owens T Induction of experimental autoimmune encephalomyelitis in C57BL/6 mice deficient in either the chemokine macrophage inflammatory protein-1α or its CCR5 receptor. Eur. J. Immunol 30, 1410–1415 (2000). [PubMed: 10820388]
31. Roscic-Mrkic B et al. Role of macrophages in measles virus infection of genetically modified mice. J. Virol. 75, 3343–3351 (2001). [PubMed: 11238860]
32. Chen Y et al. Alterations of gene expression in failing myocardium following left ventricular assist device support. Physiol. Genomics 14, 251–260 (2003). [PubMed: 12824457]
33. Gentleman RC et al. Bioconductor: open software development for computational biology and bioinformatics. Genome Biol. 5, R80 (2004). [PubMed: 15461798]
34. Wu Z, Irizarry RA, Gentleman R, Martinez-Murillo F & Spencer F A model-based background adjustment for oligonucleotide expression arrays. J. Am. Stat. Assoc 99, 909–917 (2004).
35. Smyth GK Linear models and empirical Bayes methods for assessing differential expression in microarray experiments. in Stat. Appl. Genet. Mol. Biol (2004).
36. Benjamini Y & Hochberg Y Controlling the false discovery rate — a practical and powerful approach to multiple testing. J. R. Stat. Soc. B 57, 289–300 (1995).
37. Lang R, Rutschman RL, Greaves DR & Murray PJ Autocrine deactivation of macrophages in transgenic mice constitutively overexpressing IL-10 under control of the human CD68 promoter. J. Immunol. 168, 3402–3411 (2002). [PubMed: 11907098]
38. Stephens R, Randolph DA, Huang G, Holtzman MJ & Chaplin DD Antigen-nonspecific recruitment of Th2 cells to the lung as a mechanism for viral infection-induced allergic asthma. J. Immunol. 169, 5458–5467 (2002). [PubMed: 12421921]
39. Saunders BM & Cheers C Inflammatory response following intranasal infection with *Mycobacterium avium* complex: role of T-cell subsets and gamma interferon. Infect. Immun. 63, 2282–2287 (1995). [PubMed: 7768610]
40. Flynn KJ et al. Virus-specific $CD8^+$ T cells in primary and secondary influenza pneumonia. Immunity 8, 683–691 (1998). [PubMed: 9655482]

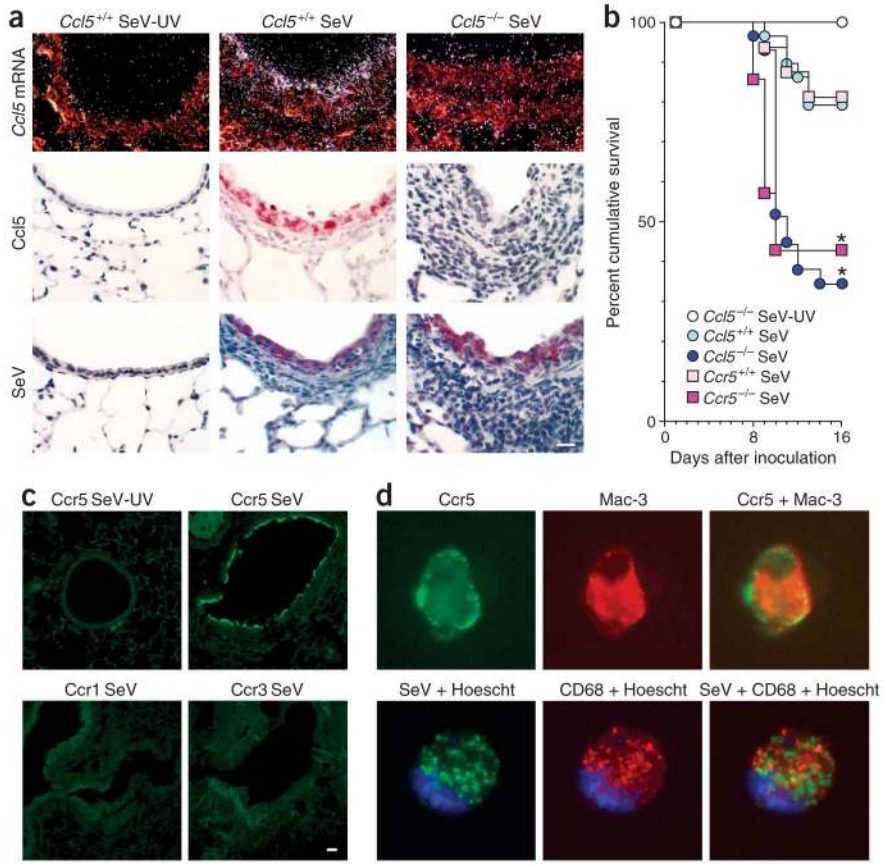

Figure 1.

Excessive airway inflammation and respiratory failure after paramyxoviral infection in *Ccl5*$^{-/-}$ mice. (**a**) *Ccl5*$^{-/-}$ and wild-type mouse lungs from day 5 after inoculation with SeV or UV-inactivated SeV (SeV-UV) were subjected to *in situ* hybridization with ^{35}S-labeled *Ccl5* cRNA or immunostained with Ccl5-specific monoclonal antibody or SeV-specific antibody. (**b**) *Ccl5*$^{-/-}$, *Ccr5*$^{-/-}$ and corresponding control mice were inoculated as in **a** and monitored for survival ($n = 29$ mice per group). * $P < 0.05$. (**c**) Mice were inoculated as in **a**, and lung sections were subjected to immunofluorescence microscopy using Ccr5-specific monoclonal antibody and FITC-conjugated secondary antibody. (**d**) Mice were inoculated as in **a**, and BAL fluid cells from day 9 after inoculation were subjected to immunofluorescence microscopy using Ccr5-specific monoclonal antibody and Mac-3–specific antibody (top row) or SeV-specific antibody and FITC-conjugated secondary antibody and CD68-specific monoclonal antibody (bottom row) as well as corresponding FITC- or Cy3-conjugated secondary antibody and Hoescht dye for nuclei. For **a**,**c** and **d**, controls for immunostaining (nonimmune IgG) and *in situ* hybridization (sense probe) gave no signal over background. Scale bars, 20 μm.

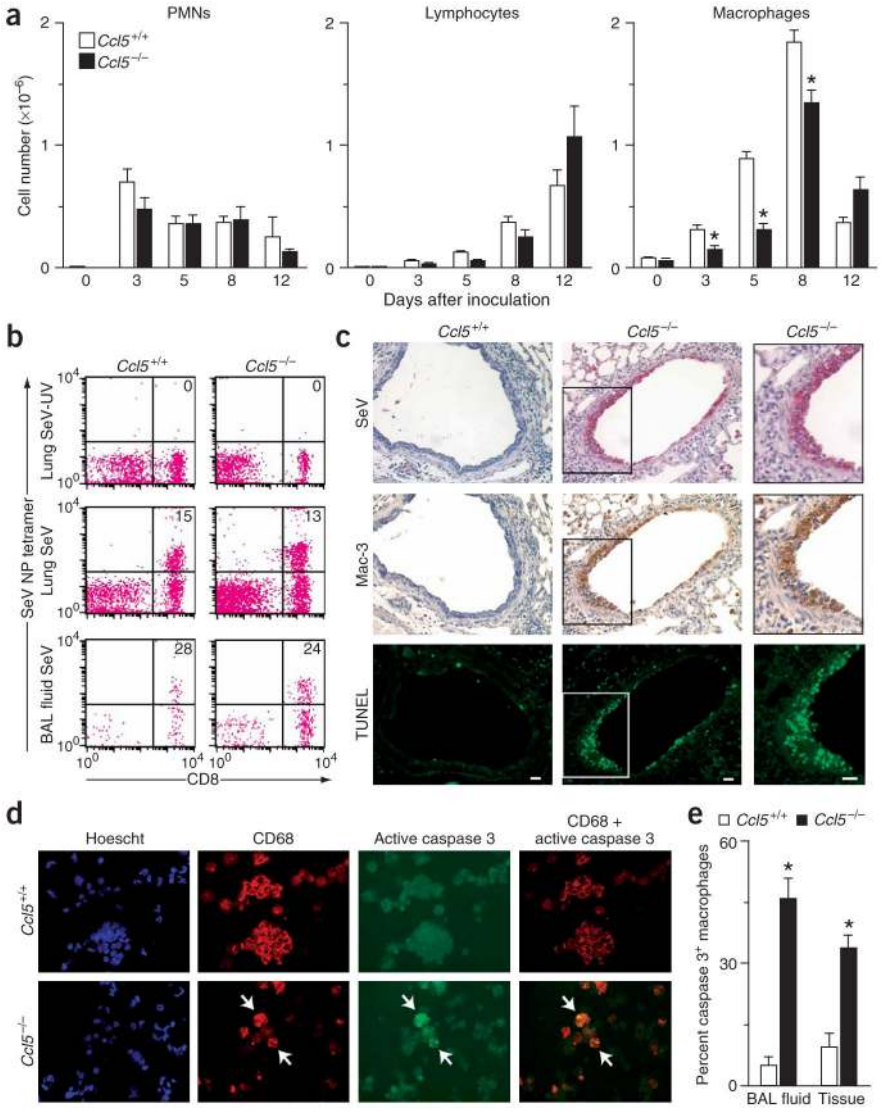

Figure 2.

Excessive macrophage apoptosis after paramyxoviral infection in *Ccl5*$^{-/-}$ mice. (**a**) *Ccl5*$^{-/-}$ and wild-type control mice were inoculated with SeV, and BAL fluid was obtained for total and differential cell counts. Values represent mean ± s.e.m. ($n = 3$). (**b**) Lung tissue and BAL fluid cells from day 12 after inoculation were used to monitor levels of CD8$^+$ and SeV$^+$ specific T cells by flow cytometry using tetrameric MHC-Sev peptide. Control analysis with tetrameric MHC-ova peptide was negative (data not shown). (**c**) Serial lung sections from day 9 after inoculation were subjected to immunostaining for SeV-specific and Mac-3–specific monoclonal antibodies and TUNEL. Scale bars, 20 μm. (**d**) BAL fluid cells from day 9 after inoculation were subjected to immunofluorescence microscopy using CD68-specific monoclonal antibody with Cy3-conjugated secondary antibody and activated caspase 3–specific monoclonal antibody with FITC-conjugated secondary antibody. Similar results were obtained for lung tissue cells (data not shown). (**e**) Quantitative analysis of results from **d**. *$P < 0.05$.

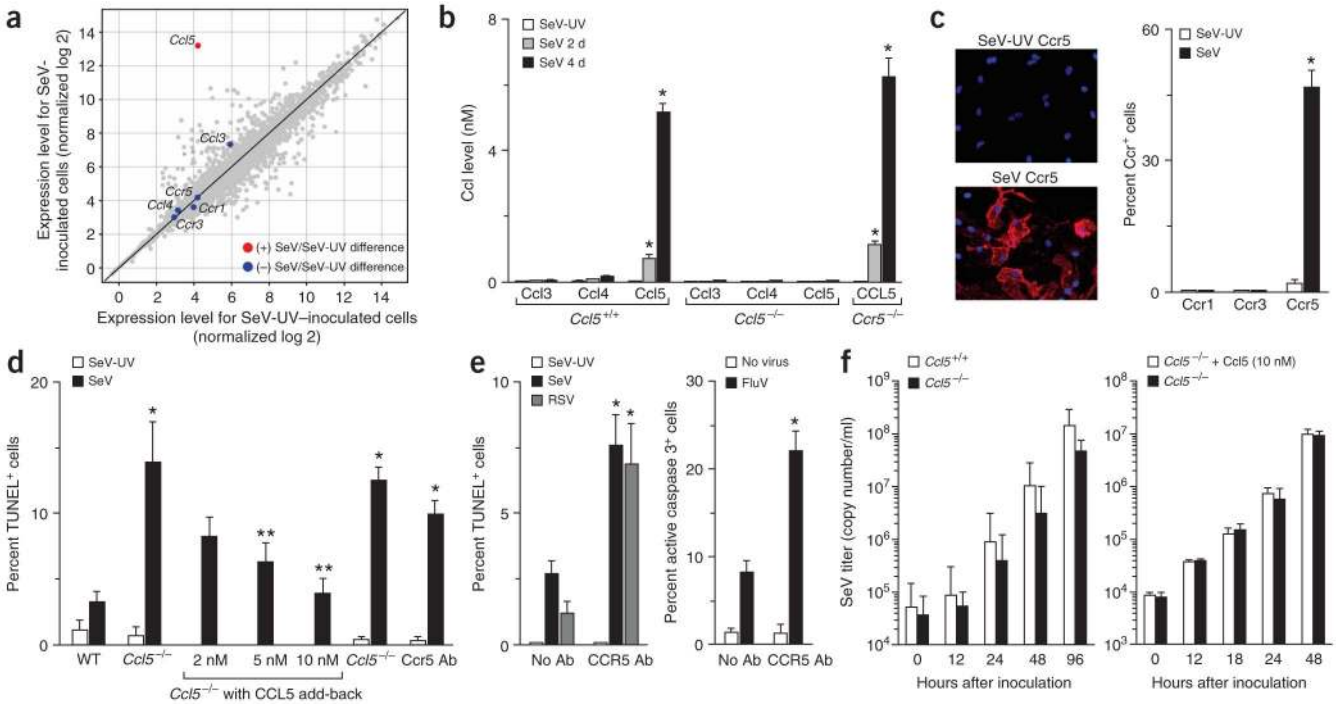

Figure 3.

Ccl5- and Ccr5-dependent protection from virus-induced apoptosis in isolated macrophages. (**a**) Wild-type mouse macrophages were infected with SeV (MOI 20) or SeV-UV, and 4 d later, cellular mRNA was subjected to oligonucleotide microarray analysis. Red circles indicate statistically significant and blue circles indicate no significant difference in SeV- versus SeV-UV–inoculated cells. (**b**) Macrophages from indicated mice were infected as in **a**, and cell supernatants were subjected to ELISA for Ccl3, Ccl4 and Ccl5 at indicated times after inoculation. (**c**) Wild-type mouse macrophages were infected as in **a** and subjected to DAPI stain and immunofluorescent stain for Ccr1, Ccr3 and Ccr5. (**d**) Macrophages from indicated mice were infected as in **a** and subjected to TUNEL at day 4 after infection. *Ccl5*$^{-/-}$ cells were also incubated with Ccl5 for 1 h before inoculation, and wild-type cells were incubated with Ccr5-specific antibody (Ccr5 Ab) from day 0 to day 4. (**e**) Human macrophages were incubated with or without CCR5-specific antibody (CCR5 Ab) and infected with SeV or respiratory syncytial virus (MOI 20) and subjected to TUNEL, or infected with influenza virus and subjected to immunostaining for active caspase 3 on day 4 after inoculation. For mouse and human cells, the same patterns were observed at days 1, 2 and 8 after infection and MOI 1–100. Control inoculation with SeV-UV gave no detectable signal for viral staining or TUNEL reaction. For **b**–**e**, values represent mean ± s.e.m. ($n = 5$). $^{*}P < 0.05$. (**f**) Macrophages from *Ccl5*$^{-/-}$ and wild-type mice were infected as in **a**, and cell supernatants were analyzed by real-time quantitative PCR for viral copy number. *Ccl5*$^{-/-}$ macrophages were also treated with vehicle or Ccl5 (10 nM) for 12 h before inoculation.

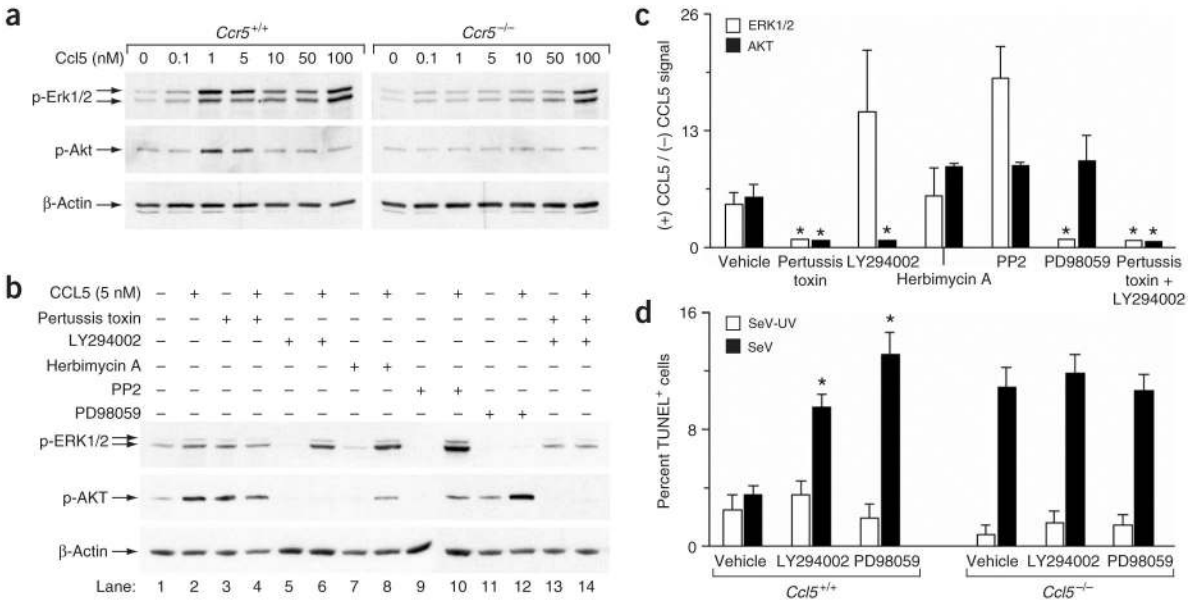

Figure 4.

CCL5 signals to $G_{\alpha i}$-PI3K-Akt and MEK-ERK pathways that block virus-induced apoptosis. (**a**) Macrophages from *Ccr5*$^{-/-}$ or wild-type control mice were incubated with Ccl5, and cell lysates were subjected to western blotting for phosphorylated Erk1/2, phosphorylated Akt or β-actin. (**b**) Human macrophages were incubated with CCL5 without or with preincubation with pertussis toxin, LY294002, PD98059, herbimycin A or PP2. Cell lysates were subjected to western blotting as in **a**. (**c**) Quantitative analysis of western blotting of human macrophages incubated with CCL5 as described in **b**. (**d**) Macrophages from wild-type or *Ccl5*$^{-/-}$ mice were inoculated with SeV or SeV-UV along with vehicle, LY294002 or PD98059 treatment, and then subjected to TUNEL 4 d later. For **c** and **d**, values represent mean ± s.e.m. *$P < 0.05$.

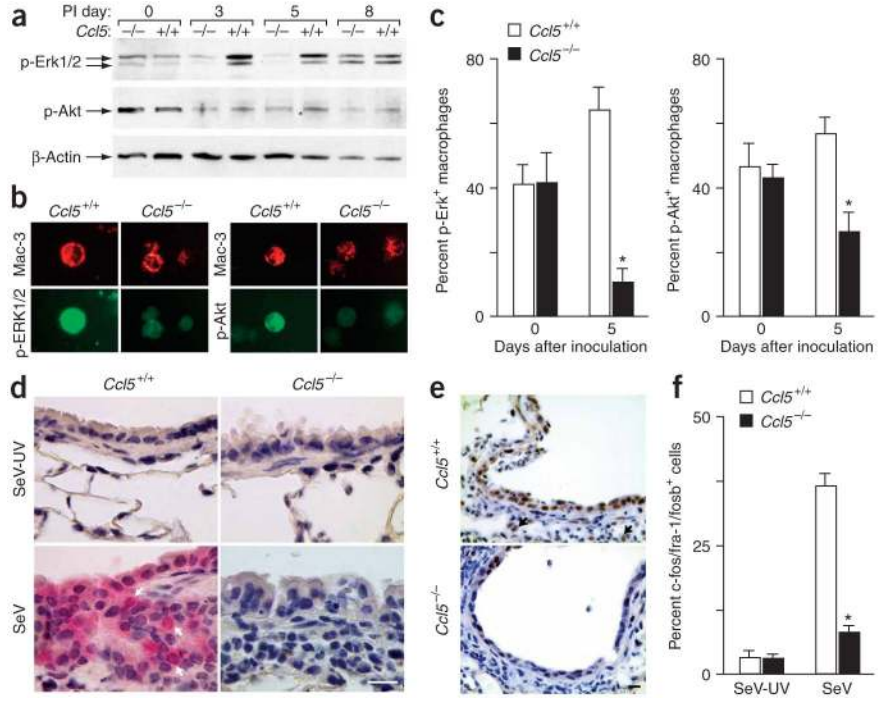

Figure 5.

Decreased activation of Akt and Erk1/2 in *Ccl5*$^{-/-}$ mice after viral infection. (**a**) BAL fluid from *Ccl5*$^{-/-}$ and wild-type mice after SeV and SeV-UV inoculation were used to prepare cell lysates that were analyzed by western blotting for phosphorylated Erk1/2, phosphorylated Akt and β-actin. (**b**) BAL fluid cells from day 5 after inoculation were also subjected to immunostaining for phosphorylated Erk1/2, phosphorylated Akt and Mac-3. (**c**) Quantitative analysis of results from **b**. (**d**) Lung sections from day 5 after inoculation were immunostained for phosphorylated Akt. Arrows indicate macrophages that immunostained positive for phosphorylated Akt. Scale bar, 20 μm. (**e**) Lung sections obtained from day 8 after inoculation were immunostained for c-fos family members. Arrows indicate macrophages that immunostained positive. Scale bar, 50 μm. (**f**) Quantification of results from **e**. Values represent mean ± s.e.m. *$P < 0.01$.

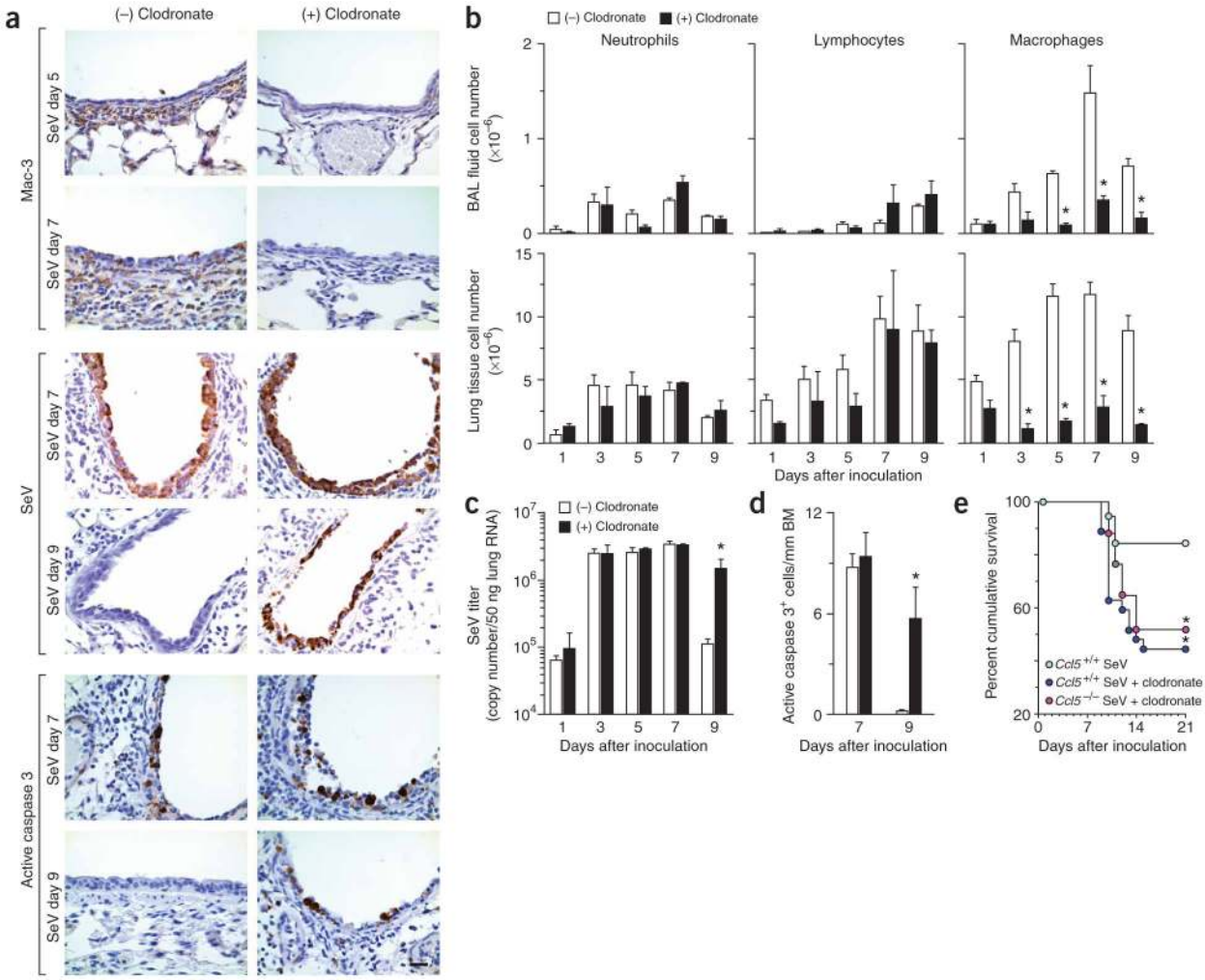

Figure 6.

Effects of macrophage depletion on viral infection in wild-type and *Ccl5*$^{-/-}$ mice. (**a**) Wild-type mice were treated with control (−) or clodronate-containing (+) liposomes. Lung sections were subjected to immunostaining for Mac-3, SeV or active caspase-3 at indicated times. (**b**) Wild-type mice were treated as in **a** and BAL fluid and lung tissue cells were obtained for total and differential cell counts. (**c**) Wild-type mice were treated as in **a**, and lung tissue samples were analyzed by realtime quantitative PCR for viral copy number. (**d**) Quantitative analysis of results in **a** for active caspase 3 immunostaining. (**e**) *Ccl5*$^{-/-}$ and corresponding control mice were inoculated and treated as in **a** and monitored for survival (n = 18–38 mice per group). *$P < 0.05$.